Journal of Liver
ISSN: 2167-0889

De León et al., J Liver 2013, 2:4
DOI: 10.4172/2167-0889.1000132

Research Article Open Access

Modulation of the Hepatic Lipidome and Transcriptome of Apoe$^{-/-}$ Mice in Response to Smoking Cessation

Héctor De León*, Stéphanie Boué, Manuel C Peitsch and Julia Hoeng

Philip Morris International R&D, Philip Morris Products S.A., Switzerland

Abstract

Hepatic lipid metabolism is profoundly affected by cigarette smoke; which likely contributes to the atherogenic plasma lipid profile observed in cigarette smokers. There is, however, a paucity of data on the identification of molecular networks and mechanisms responsible for the reduction of cardiovascular risk in former smokers compared to the risk of current smokers.

Using ApoE$^{-/-}$ mice, an experimental model exhibiting a high atherogenic rate that leads to rapid development of vascular lesions, we investigated the effects of discontinuing smoke exposure on both hepatic lipid and transcriptome profiles. Livers from ApoE$^{-/-}$ mice exposed to: (i) mainstream smoke of the reference research cigarette 3R4F for six months (CS), (ii) fresh air for six months (sham-exposed), or (iii) CS for three months followed by fresh air for three months (cessation), were extracted and their lipid composition analyzed on six different mass spectrometry platforms. Targeted and non-targeted mass spectrometry methods allowed quantification of more than 200 lipid species. The liver transcriptomes of the same animals were profiled using Affymetrix arrays.

With the exception of triacylglycerols (TAGs), most lipid species that were elevated in liver as a result of cigarette smoke exposure were decreased during the smoking cessation protocol. They included free and esterified cholesterol, phospholipids, sphingomyelins, and ceramides. The hepatic concentration of TAGs was higher in the cessation group as compared to the sham or CS groups. Gene Set Enrichment Analysis (GSEA) of the transcriptomes of the three experimental conditions revealed key hepatic functions affected by CS exposure and smoking cessation, including glutathione metabolism, oxidoreduction, and lipid biosynthesis. A subset of mice across the three experimental groups displayed up-regulation of a set of genes consistent with an exocrine pancreas signature.

Investigating the simultaneous changes on the hepatic lipidome and transcriptome in a murine model of atherosclerosis enabled the characterization of a liver-specific profile in response to smoking cessation. This information supports our efforts to develop an integrative model of key metabolic changes induced by cigarettes smoke and smoking cessation in tissues relevant to atherogenesis, including blood vessels, adipose tissue and liver.

Keywords: Smoking cessation; Atherosclerosis; Apoe$^{-/-}$ mice; Smoking; Transcriptomics; Lipidomics; Liver; Lipid Metabolism; Cholesterol synthesis

Introduction

Cigarette Smoke (CS) evokes a wide range of responses in the liver, from induction of drug-metabolizing enzymes to tissue fibrosis and exacerbation of nonalcoholic fatty liver disease [1-3]. CS is also a known risk factor for the development of cardiovascular disease as determined by surrogate plasma markers of inflammation and traditional risk factors including dyslipidemia [4,5]. Despite extensive clinical research on the association of Low- and High-Density Lipoprotein (LDL and HDL) levels with cardiovascular risk, a proportion of patients optimally treated with statins remain at a high risk [6, 7]. The high cardiovascular risk in this patient group is a reminder of the complexity of a polygenic syndrome where numerous atherogenic molecular entities contribute to plaque development. As the ultimate metabolic organ, the liver plays a major role in synthesizing and maintaining homeostatic levels of many plasma mediators and lipoproteins (e.g., LDL, VLDL) that may be either associated with or mechanistically involved in vascular lesion formation. Drawing such distinction for a large number of molecular entities using conventional research tools represents a sizable challenge. Omics technologies and biological network models enable the integration of large diverse datasets and have begun to provide new insights into the underlying vascular pathobiology.

The overarching goal of this study was to investigate the molecular effects of mainstream CS exposure and smoking cessation on hepatic, vascular and respiratory tissues of ApoE$^{-/-}$ mice using a systems-wide biology approach. We hypothesized that CS-dependent effects are progressively deactivated upon smoking cessation. Using state-of-the-art omics technologies, we have investigated the effects of smoke exposure and cessation on the hepatic and vascular lipidomes as well as on the liver transcriptome of ApoE$^{-/-}$ mice, a model of human atherosclerosis [8]. We have previously reported on a study in which we exposed three groups of ApoE$^{-/-}$ mice to i) CS for six months (continuous exposure group), ii) CS for three months followed by three months of fresh air (cessation group) and iii) fresh air for six months (sham exposure group) [9,10]. In the continuous exposure group, we have examined the plasma, vascular and hepatic lipidome and reported on their numerous changes [9]. The CS-induced vascular changes included accumulation of Ceramides (Cer), Cholesteryl Esters (CE) and Phosphatidyl Choline (PC) species, whereas the hepatic effects encompassed changes in Free and Esterified Cholesterol (FC and CE),

***Corresponding author:** Héctor De Leon, CV Systems Toxicology, Biological Systems Research, Philip Morris International R&D, Quai Jeanrenaud 5, 2000, Neuchâtel, Switzerland, Tel: +41 (0)58 242 2571; E-mail: hector.deleon@pmi.com

Received October 07, 2013; **Accepted** November 13, 2013; **Published** November 20, 2013

Citation: De León H, Boué S, Peitsch MC, Hoeng J (2013) Modulation of the Hepatic Lipidome and Transcriptome of Apoe$^{-/-}$ Mice in Response to Smoking Cessation. J Liver 2: 132. doi:10.4172/2167-0889.1000132

Triacylglycerols (TAG), Phospholipids (PL), Sphingomyelins (SM) and Cer. The plasma changes were mainly characterized by increases in SM and Sphingosine-1-Phosphate (S1P) [9].Furthermore, we reported that the plasma of mice of the cessation group displayed lower levels of all lipid classes examined when compared to the exposure group[10]. We also observed that smoking cessation hindered the CS-dependent retention rates of atherogenic lipid classes in vascular tissue [10]. Here, we report on the effects of smoking cessation on the hepatic lipidome, which resulted in a mixed pattern where concentrations of certain lipids, including SM and FC, were decreased, whereas TAGs were responsible for an overall increase in hepatic lipid content. We performed this analysis in animals from the same experiment used to demonstrate the atherogenic effects of CS exposure [9] and smoking cessation [10]. Gene expression profiling of the liver tissue of the cessation group indicated that the number of differentially regulated genes was considerably lower when compared to the continuous exposure group. Our data indicate that smoking cessation resulted in a hepatic profile exhibiting lower concentrations of atherogenic molecules and an increased metabolic capacity.

Materials and Methods

Animals

We have previously described in detail most methods used in this report [9]. Animal procedures were in conformity with the AALAS Policy on the Humane Care and Use of Laboratory Animals (AALAS, 1996) and were approved by the Institutional Animal Care and Use Committee (IACUC). Female ApoE$^{-/-}$ (ApoE/Bom, B6.129P2-Apoe^{tm1Unc}N$_{11}$) mice aged 5-9 weeks were obtained from Taconic (Denmark & USA). Animals were fed a normal chow diet based on soybeans with 0.003% cholesterol and 4% fat (2014 Teklad) from Harlan (Oxon, UK). Filtered tap water was supplied *ad libitum* and changed daily. Exposure room was maintained at 21.8 ± 0.5 ˚C and at a relative humidity of 54.7 ± 3.5%. Mice were observed daily for mortality, morbidity, and signs of overt toxicity or injury. Body weight was measured at least once per week during the exposure period.

Experimental design

ApoE$^{-/-}$ mice were exposed to filtered fresh air (sham exposure group) or to mainstream CS for three and six months (continuous exposure group) or for three months only and then switched to sham exposure for three additional months (cessation group). Data from the sham and continuous exposure groups were previously reported [9]; for comparison purposes, they are also included in this report. The protocol was designed to model the effects of smoking cessation. Seven to eight mice were used for lipid measurements in the liver.

Smoke generation and animal exposure

The reference cigarettes (3R4F) were obtained from the Tobacco Research and Development Center (University of Kentucky, KY, USA). Smoking parameters including puff duration and volume were conducted in conformity with the Health Canada Intense (HCI) smoking regimen [11] as previously described [9]. Animals were exposed to fresh filtered air or CS using whole-body exposure polycarbonate cages. Total Particulate Matter (TPM) levels for CS-exposed groups were targeted at 600 µg/l. The exposure regimen consisted of three 1-hour periods a day and 30-minute intervals with fresh filtered air, five days a week for up to six months. Plasma carboxyhemoglobin (COHb) levels were determined as a marker of smoke uptake at three and six months, as described elsewhere [12].

Test atmosphere characterization

To ensure reproducibility of the smoke generation, analyses of the test atmosphere were conducted regularly during the study. Analytical methods for each component including TPM, Carbon Monoxide (CO), nicotine, aldehydes and particle size distribution have been previously described [12]. Test atmosphere parameters for this study have been summarized elsewhere [9].

Quantification of nicotine metabolites

Nicotine metabolites were measured in 16-h urine samples and have been previously published [9]. Briefly, trans-3'-Hydroxycotinine (3'HOCOT), Nornicotine (NNIC), Norcotinine (NCOT), Cotinine (COT) and Nicotine-N'-oxide (NN'O) were quantified by High-Performance Liquid Chromatography (HPLC) after derivatization with 1,3-diethyl-2-thiobarbituric acid according to Rustemeier et al [13].

Lipidomics analysis

Molecular lipids from liver were extracted and quantified by mass spectrometric analysis by Zora Biosciences (Espoo, Finland [14]) using synthetic non-endogenous standards as described in detail in Boue et al [9]. The mass spectrometry data files were processed using Lipid Profiler™ and MultiQuant™ 2.0 Software to generate a list of lipid names and peak areas. Lipids were normalized to their respective internal standard and tissue weight. The concentrations of molecular lipids are presented as nmol/mg wet tissue. Lipid nomenclature and categorization used (Table 1) followed the 2009 update of the LIPID MAPS system [15].

Transcriptomics analysis

RNA preparation: Total RNA was extracted from homogenized liver using TRIzol™ and quantified using the Nanodrop ND-1000 (peqlab); RNA integrity was determined using the Agilent 2100 Bioanalyzer, Microarray preparation. Transcriptome analysis was done following the manufacturer's recommendations in the GeneChip® HT 3' IVT Express Kit (Santa Clara, CA) guide. Ten µg of biotinylated fragmented cRNA was hybridized to AffymetrixGeneTitan: GeneChip™ HT MG-430 PM for 16 hours. HT Array Plates were scanned using the HT Scanner (AffymetrixGeneChip™ HT). Scanned image files were visually inspected for artifacts before being analyzed.

Gene expression data analysis: Raw RNA expression data for each data-set were analyzed using the affy and limma [16,17] packages of the Bioconductor suite of microarray analysis tools [16] available for the R statistical environment [18]. Robust Microarray Analysis (RMA) background correction and quantile normalization were used to generate microarray expression values [19]. An overall linear model was fit to the data for all sample groups, and specific contrasts of interest were evaluated to generate raw p-values for each probe set on the expression array [17]. The Benjamini-Hochberg False Discovery Rate (FDR) method was then used to correct for multiple testing effects.

Partial least square discriminannt analysis (PLS-DA): PLS-DA was applied on filtered gene expression profiles (removing constant profiles and low expressed probesets) using the 'plsda' function of the caret package [20].

Gene set-Based Expression Analysis. GSEA [21] was performed using the Confero platform [22] with further developments. For each pairwise contrast described above, probe sets were mapped onto Entrez Gene identifiers and collapsed to remove the multiple probe set-to-gene mappings using the Confero platform [22]. GSEA was

Lipid MAPS ontology			LIPID_CLASS
Glycerolipids	Diradylglycerols	Diacylglycerols	DAG
	Triradylglycerols	Triacylglycerols	TAG
Glycero-phospholipids	Glycerophosphocholines	1-(1Z-alkenyl),2-acylglycerophosphocholines	PC P
		1-(1Z-alkyl),2-acylglycerophosphocholines	PC O
		Diacylglycerophosphocholines	PC
		Monoacylglycerophosphocholines	LPC
	Glycerophosphoethanolamines	1-(1Z-alkenyl),2-acylglycerophosphoethanolamines	PE P
		1-(1Z-alkyl),2-acylglycerophosphoethanolamines	PE O
		Diacylglycerophosphoethanolamines	PE
		Monoacylglycerophosphoethanolamines	LPE
	Glycerophosphoglycerols	Diacylglycerophosphoglycerols	PG
	Glycerophosphoinositols	Diacylglycerophosphoinositols	PI
	Glycerophosphoserines	Diacylglycerophosphoserines	PS
Sphingolipids	Ceramides	Ceramides	Cer
	Neutral glycosphingolipids	GalNAcβ1-3Galα1-4Galβ1-4Glc- (Globo series)	Gb3
		Simple Glc series	Glc/GalCer
			LacCer
	Phosphosphingolipids	Ceramide phosphocholines (sphingomyelins)	SM
Sterol Lipids	Sterols	Free Cholesterol	FC
		Steryl esters	CE

Table 1: Lipid classes nomenclature according to Lipid Maps.

performed by ranking genes by their respective t-statistic, calculated using the Limma package, on the MSigDB [21] collection of canonical pathways (Cp collection including KEGG, Reactome and Biocarta pathways) in the curated gene sets (C2), as source of prior biological knowledge. While significant results were obtained for the continuos smoke exposure vs. sham exposure comparison at six months with a FDR<0.01 [9], no significant results were obtained for the cessation vs. sham exposure comparison. Therefore, we present here GSEA results for the latter comparison using a more permissive FDR threshold (<0.1). To facilitate and accelerate the interpretation of GSEA results, gene sets were clustered and visualized in the form of a network using a similar method to the one used in the Enrichment Map [23]. Briefly, our approach enabled to group gene sets based on common underlying leading edge genes corresponding to the core genes contributing to the maximum enrichment scores. For a given contrast, the Jaccard distance was computed between each significant gene set pair. The Jaccard distance was converted into similarity matrix (1-Jaccard) used as input for APcluster, a powerful algorithm enabling to cluster gene sets in rich-club and communities [24]. The results were visualized in the form of a network revealing communities of gene sets representative of perturbed biological processes/pathways in a specific pairwise contrast. Each community and rich club was then annotated using DAVID 6.7 [25] functional clustering function with the union of all leading edge genes of the gene sets present in a community or a rich club. The network of gene sets was visualized using Cytoscape [26], with the edges length being proportional to the Jaccard distance between gene sets.

Correlation of liver lipidomics and transcriptomics

Lipidomics and transcriptomics were performed on liver samples of the same mice. Therefore, it was possible to establish correlations between the lipidomics and transcriptomics profiles with data from each liverin all experimental groups; seven mice exposed to filtered air for six months (sham exposure group), eight mice exposed to CS for the same period (continuous exposure group), and eight mice exposed to CS for three months followed by three months of cessation (cessation group). Missing values from the lipidomics data were replaced by zero. Profiles were correlated using the correl function in R. Pairs of probesets and lipid species which showed absolute correlation coefficient above 0.8 were further analyzed using DAVID 6.7 [25]. In addition, focused analyses of lipid metabolism-related pathways and genes of interest were conducted using NextBio [27].

Statistical analysis

Data are expressed as mean ± Standard Error of the Mean (SEM), unless otherwise indicated. Differences between group means for non-lipidomics data (plasma lipoproteins, plaque area and aortic total cholesterol) and their associated 95%-Confidence Interval (CI), as estimated by the Fisher's Least Significant Difference (LSD) method, were obtained. All computations were performed with SAS version 9.2 (SAS Institute Inc., Cary, NC, USA). For lipidomics data, Wilcoxon rank-sum tests were performed for pairwise comparisons and statistical significance (unadjusted p-value < 0.05) reported.

Results

The lipidomics and transcriptomics profiles of the smoking cessation group were compared to those of the continuous exposure group. The three groups (sham exposure, continuous exposure and cessation) represent separate arms of a single experimental design with well-defined exposure and cessation protocols. Previously reported data on smoke exposure [9] was included in the current report to provide context to the novel findings on the effects of smoking cessation compared to continuous and sham exposure.

Smoking cessation resulted in lower levels of most hepatic lipid classes compared to continuously smoke-exposed and sham animals

Continuous exposure to CS resulted in increased levels of most lipid classes in the liver as we have previously reported [9] (Figure 1, panel A). The concentrations of most of those lipid classes were lower in the smoking cessation groupwhen compared to continuous exposure to CS. (Figure 1, panel B). However, CE and Glycerolipids (GL) levels were increased in the cessation group when compared to

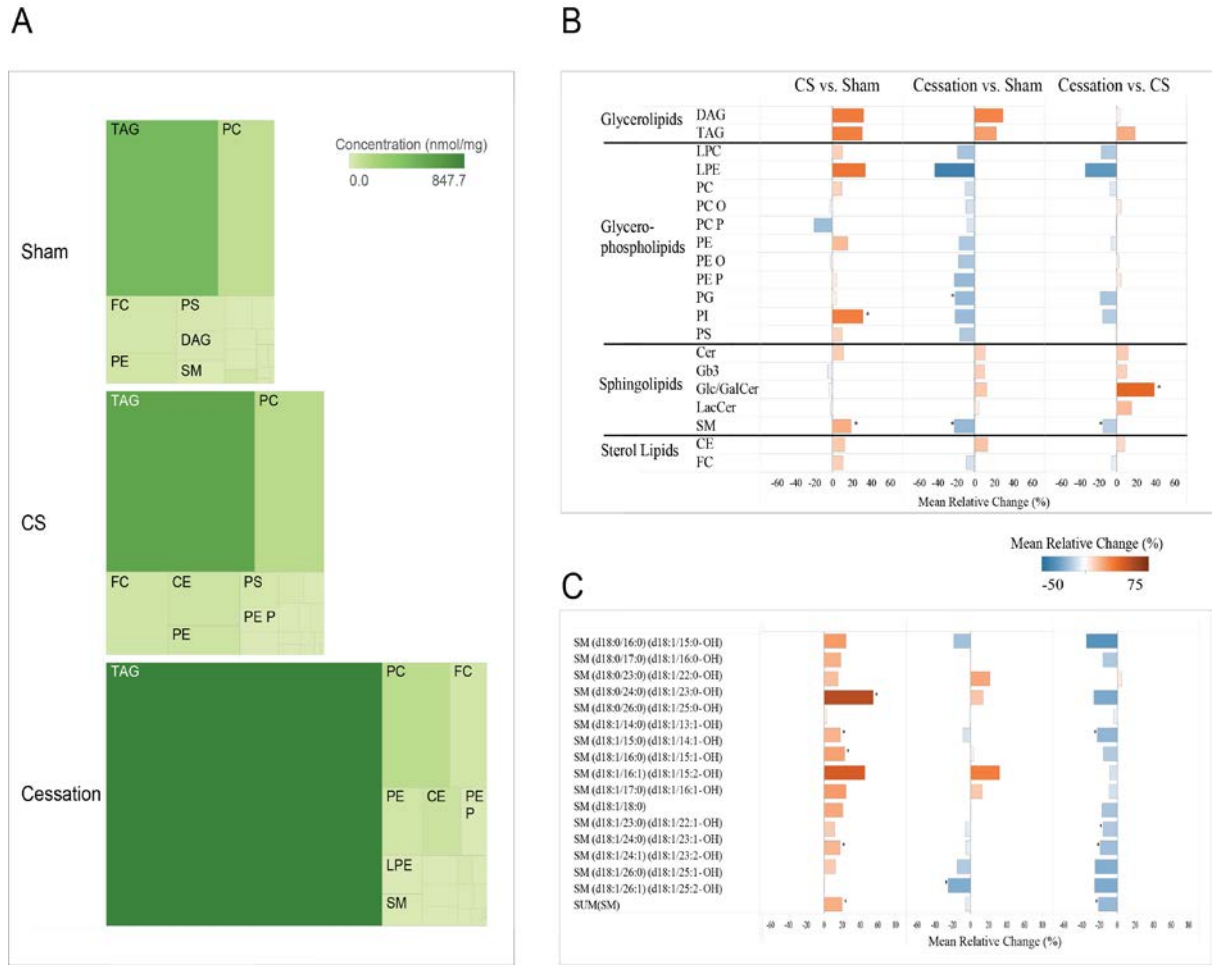

Figure 1: Hepatic lipid regulation: Changes in hepatic lipid classes in continuous CS exposed (CS) and smoking cessation (cessation) groups.
A. The absolute concentration of lipids measured in each lipid class is shown as a tree-map representation where the size of the box is proportional to the concentration.
B. Percentage differences in lipid class concentrations in ApoE$^{-/-}$ mice liver between CS or cessation and sham exposure groups (CS vs. sham, cessation vs. sham) and cessation and CS-treated groups (cessation vs. CS). The relative mean change between groups is indicated as the length and color of the bars.
C. Changes on specific Sphingomyelin (SM) lipid species. The SUM of a lipid class represents the total concentration or changes of all molecular species.

the continuous and sham exposure groups. Lipid classes that exhibited lower levels upon smoking cessation compared to continuous exposure included Free Cholesterol (FC), Phosphatidylcholine (PC), Phosphatidyl Ethanolamine (PE), plasmalogens (alkyl- and alkenyl-linked PC and PE), Phosphatidylserine (PS), Lyso PC (LPC), LysoPE (LPE), Phosphatidylglycerol (PG) and SM. Concentrations of Cer, lactosyl ceramide (LacCer), glucosyl/galactosyl ceramide (Glc/GalCer) and globotriaosylceramides (Gb3) were slightly increased upon smoking cessation compared to continuous or sham exposure. Analysis of the changed SM species showed that five molecular species (e.g. SM (d18:1/14:0) (d18:1/25:0-OH)) were responsible for the changes. Virtually all molecular species returned to lower levels compared to continuous exposure; however, four of them remained high when compared to the sham-exposed group (Figure 1, panel C).

TAGs represented not only the lipid class with the largest concentration levels within GLs but also the largest concentration of all lipids examined (Figure 1, panel A). TAGs were increased by continuous CS exposure and their levels were even higher upon smoking cessation (Figure 1, panels A and B). Individual animal levels of hepatic TAGs in the smoking cessation group showed a wider range of concentrations than those observed in livers from animals of the sham exposure and cessation groups (Figure S1). The pool of TAGs comprised molecules with carbon chains spanning from 14 to 22 carbons, for total carbon chains of 48-58 within a single TAG molecule. Most molecular structures contained unsaturated fatty acids (1-10 unsaturated bonds). CS induced a pattern of lipid accumulation characterized by molecules with large total carbon chains (54-58 total carbons per TAG molecule) irrespective of the number of unsaturated bonds. This pattern was entirely different from the one exhibited by smoking cessation when compared to continuous exposure (Figure 2, right panel). Compared to sham exposure, smoking cessation resulted in increased levels of virtually all TAGs containing total fatty acid carbon chains of 50-58 (Figure 2, center panel).

The smoking cessation protocol rendered a hepatic gene expression pattern centered on lipid metabolism and a lower atherothrombotic potential

The gene expression profile of livers from single ApoE$^{-/-}$ mice conducted after six months after CS exposure and three months of CS exposure followed by three months of cessation is depicted in Figure 3 as volcano plots (compared to sham mice). Amplitude (x axis, log2 fold change) and significance (y axis, log10 of adjusted p-value (FDR))

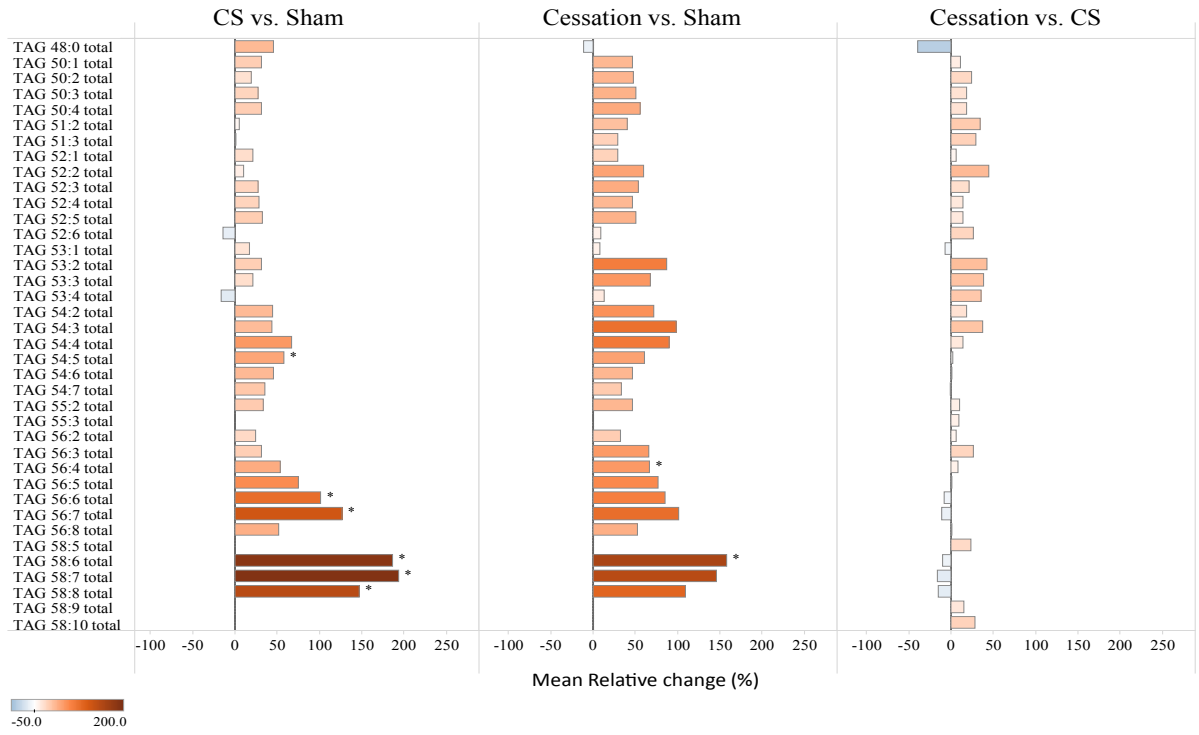

Figure 2: Hepatic regulation of TAGs: Percentage differences in TAG class concentrations in ApoE$^{-/-}$ mice livers between the CS- or cessation and sham-treated groups and cessation and CS-treated groups as defined in Figure 1. The relative mean change between groups is indicated as length and color of the bars.

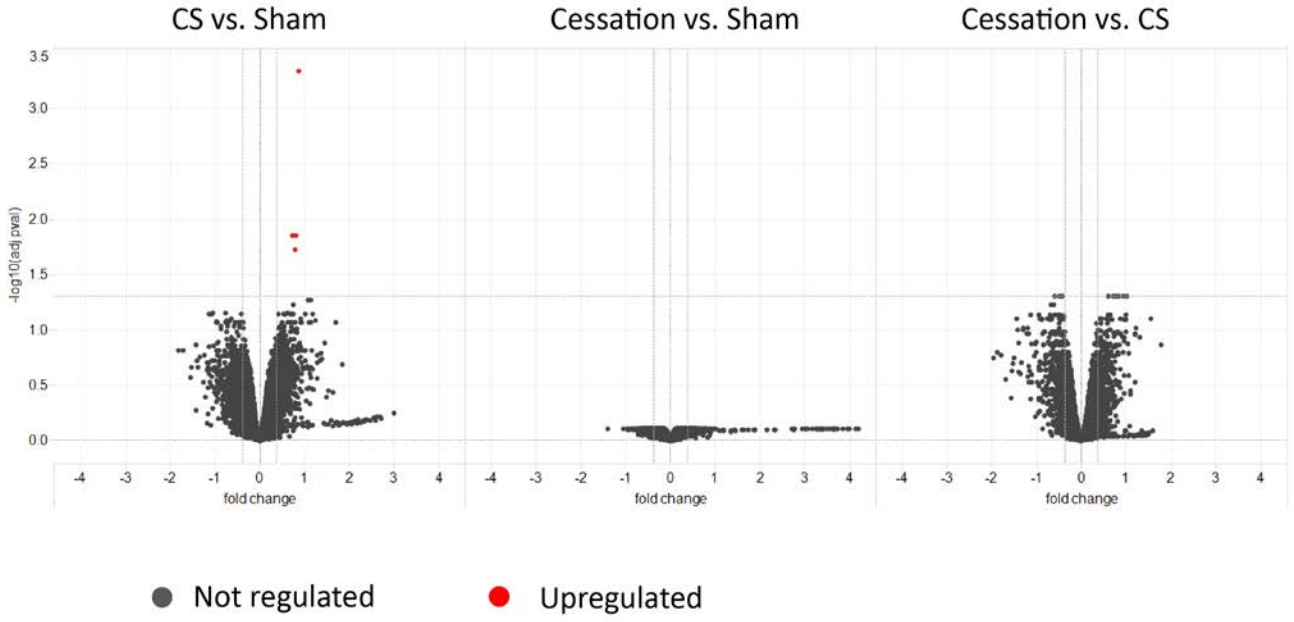

Figure 3: Hepatic gene expression after six months exposure to CS or to the smoking cessation protocol: Volcano plots representing all probe sets that are not constant in the experimental groups. Red dots represent probe sets that were statistically significantly up-regulated after multiple testing corrections. Left panel compares CS vs. sham exposure groups at six months; middle panel compares cessation vs. sham group, whereas right panel depicts a comparison of cessation vs. CS group. The rectangles in the left and central panels include a set of genes that were clearly up-regulated but exhibited low significance values. Further examination of these probes using DAVID revealed that these genes were also highly expressed in other gastrointestinal organs (e.g. pancreas, stomach) with the pancreas exhibiting a signature with 63% similarity.

depict gene expression changes in the livers of the three groups. This analysis included liver samples from seven to eight animals per group that passed the quality control requirement for gene expression analysis. The vast majority of genes were unchanged after smoking exposure. Only a small set of genes were statistically significantly up-regulated (Figure 3, left panel). The genes up-regulated by continuous smoke exposure included Zfp385b, a transcription factor lacking a well described function, Cyp1a2, a detoxifying enzyme, Slc2a9, a facilitated glucose transporter, and Tk1, a thymidine kinase particularly active in proliferating cells. Compared to sham exposure, smoking cessation also exhibited a relatively unchanged pattern of gene expression, except that the genes up-regulated by continuous exposure exhibited non-significant values in the smoking cessation group (Figure 3, right panel).

Continuous CS exposure induced the expression of numerous genes within canonical pathways involved in *GSH* metabolism (RC6), oxidoreduction (RC4), lipid biosynthesis(RC11) coenzyme biosynthesis (RC16) and phosphorus metabolic process (RC18), as revealed by gene set enrichment analysis (GSEA, FDR <0.01) [9]. This scenario was consistent with CS-mediated induction of drug metabolizing enzymes (phase I and phase II conjugation); enzymes involved in lipid metabolism (both catabolic and biosynthetic pathways), as well as phosphorylation pathways. GSH transferase activity was a perturbed pathway and so was the Tricarboxylic Acid (TCA) cycle. GSEA of gene expression data in the cessation group showed no significant gene sets (FDR <0.01). However, relaxing the FDR from <0.01 to <0.1 resulted in the identification of a collection of regulated genes within families related to response to hormone stimulus (RC1), lipid biosynthesis (RC2), translation (RC7), nucleic acid metabolism (RC6) and phosphorus metabolic processes (RC8) (Figure 4). Within the latter (RC8), pathways involved in hemostasis and platelet activation had a predominant representation and was all down-regulated. Similarly, nucleic acid metabolism included a rich network of genes related to various phases of the cell cycle (e.g., G1-S transition) including cyclins (e.g., E, A) as well as Cdc- and P53-related genes; the vast majority of these pathways were also down-regulated. In contrast, genes involved in cholesterol biosynthesis were up-regulated within the RC2 family of pathways (Figure 4).A DAVID-based analysis of the probe sets whose profiles best correlated with lipid profiles (correlation coefficients>0.8) indicated a mixed, not fully discernible structural or functional

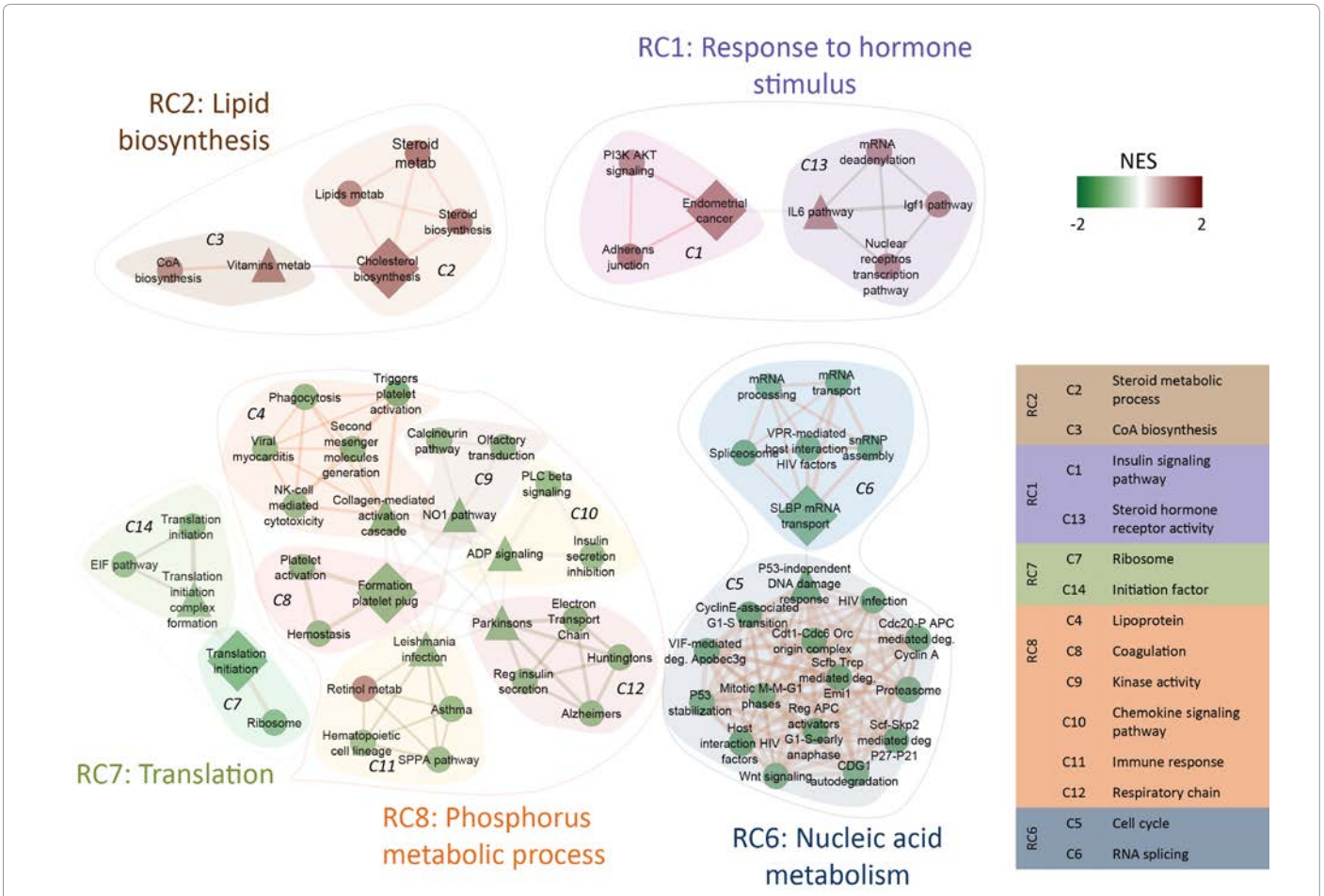

Figure 4: Gene Set Enrichment Analysis (GSEA) of hepatic transcript profiles in the cessation group compared to the sham group: Each node represents a gene set from the Canonical Pathways (Cp) collection of MSigDB which is significantly enriched in the comparison cessation vs. sham after six months exposure in liver samples (FDR<0.1). Gene sets are grouped based on the genes they share that contribute to the enrichment score of the dataset. Color of the nodes as well as font size of node labels is proportional to the normalized enrichment score. Nodes representative of their Community (C) are depicted as triangles and nodes representative of their Rich Club (RC) are represented as diamonds. Annotation of each C and RC is done using the functional annotation clustering tool of DAVID with the list of genes from the C or RC contributing to the enrichment score (leading edge genes).

clustering pattern. The lack of significant functional gene categories may be due to the small number of probe sets that made the 0.8 coefficient cutoff (66 probe sets). Nonetheless, the resulting categories closest to statistical significance revealed pathophysiological clues that deserve further analysis. Three gene categories involved in lipid metabolism, fatty acid transport and macrophage-mediated immunity exhibited the lowest p-values (Tables S3 and S4).

A subset of livers from ApoE$^{-/-}$ mice exhibited up-regulation of a set of genes consistent with an exocrine pancreas signature

The comparison of gene expression data between the cessation and sham exposure groups revealed a set of genes that were clearly up-regulated but were below the significance threshold when analyzed as a group (Figure 3, central panel). Closer inspection of single animal data for the probe sets with a cessation vs. sham exposure log fold-change ratio > 1 indicated that a highly significant up-regulation of the hepatic gene set was observed only in a selected number of mice within each group. One animal in the sham exposure group and three and five animals in the continuous exposure and cessation groups showed similar levels of up regulation, whereas two additional mice from the continuous exposure group exhibited a significant but lower degree of up-regulated expression (Figure 5). PLS-DA calculated using the transcriptomics profiles and the three exposure groups identified the mice with the highest levels of expression as a relatively well delimited single cluster (Figure S2).

A search of murine tissues where these hepatic genes are usually regulated and/or highly expressed was conducted using DAVID (http://david.abcc.ncifcrf.gov/home.jsp). This analysis revealed that mouse pancreas exhibited the highest percentage of similar genes (63%), followed by other gastrointestinal organs including stomach (22%), spleen (22%) and colon (22%) (Table 2). The set of hepatic genes with a pancreatic signature included pancreatic amylase (Amy2a), chemotrypsin-like elastase (Cela3b), Carboxipeptidase B1 (Cpb1) and Pancreatic lipase (Pnlip). A complete list of the 49 genes with a log ratio cessation vs. sham exposure> 1 is provided in Table S1 and the

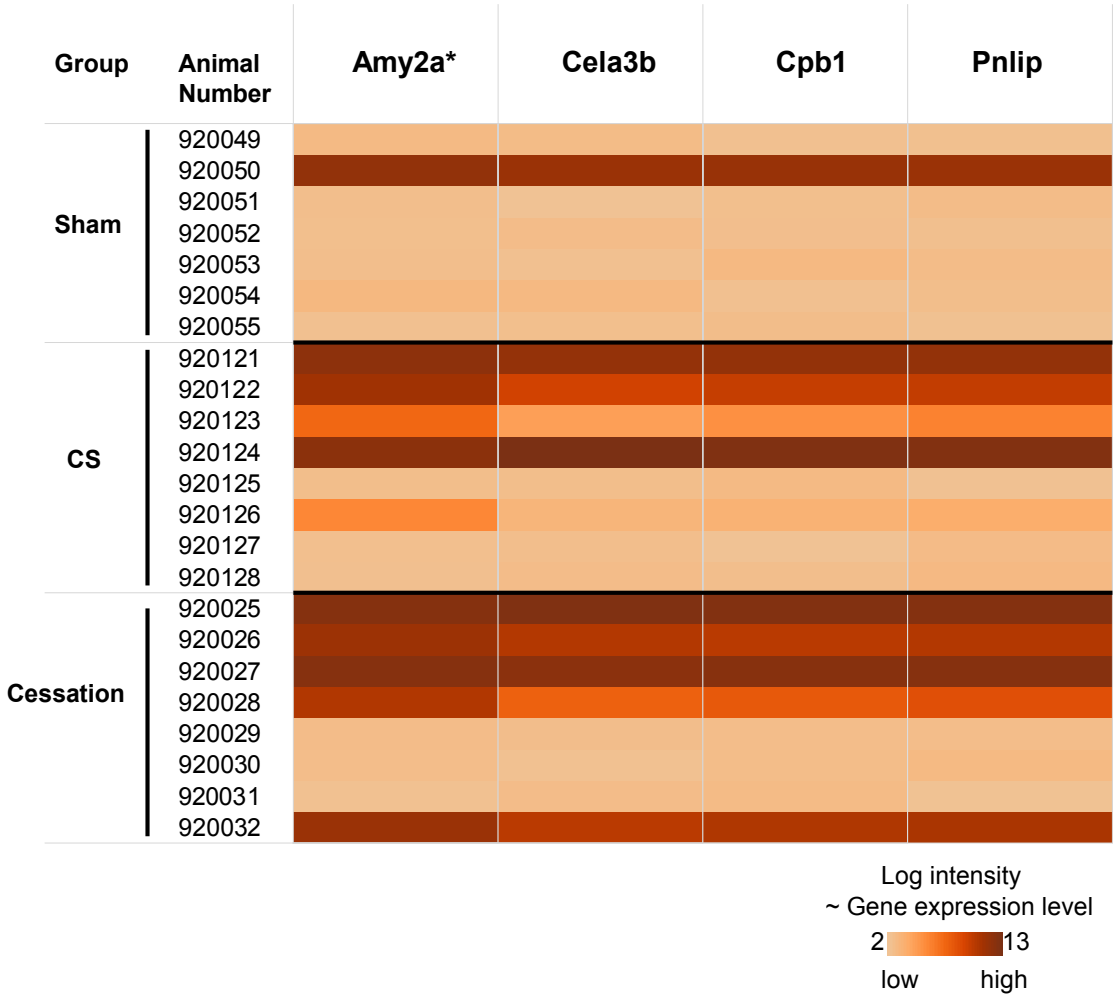

*The probeset monitors multiple members of the Amy2a gene family, namely Amy2a1, Amy2a2, Amy2a3, Amy2a4, Amy2a5.

Figure 5: Pancreatic gene expression signature detected in livers of ApoE$^{-/-}$ mice: Heat map of gene expression levels (log 2 intensity level calculated by rma) for selected genes shown in Figure 3 for each mouse of all groups. Color intensity is proportional to the intensity of the spot on the microarray and reflects gene expression level of each gene. Animal Number (AN) is given for each mouse. Each gene is represented by one probe set present on the microarrays. The set of hepatic genes with a pancreatic signature comprised a set of 48 genes of which pancreatic amylase (Amy2a), Chemotrypsin-like elastase (Cela3b), Carboxipeptidase B1 (Cpb1) and Pancreatic lipase (Pnlip) are shown.

expression levels of the entire set of genes and the mice number and IDs within each group are listed in Table S2.

A correlative analysis of the hepatic transcriptomic and lipidomic profiles from single animals was conducted for all genes and lipid classes examined. Probe sets with a correlation coefficient >0.8 are shown in Figure 6.

Discussion

Exposure to CS increases the risk of cardiovascular, liver and lung diseases [1,4,5]. Our biological network models [28,29], as well as the use of ApoE$^{-/-}$ mice to recreate human atherosclerotic [9,10,30,31] and emphysematous changes [32] have provided valuable mechanistic clues to deepen our understanding of the pathologies related to cigarette smoking. Data from the present work and some of our previous reports [9,10,32] using state-of-the-art omics technologies to examine the molecular changes induced by CS exposure and smoking cessation were derived from a single large study in ApoE$^{-/-}$ mice. Our previous findings indicate that CS exposure accelerates the development of vascular lesions and emphysema in ApoE$^{-/-}$ mice [9,32], an animal model that is genetically prone to develop dyslipidemia and atherosclerotic plaques [33]. Body weight of animals increased after smoking cessation, a common finding observed in mice under a cessation protocol and in humans who quit smoking. It is well known that smoking cessation is accompanied by an increase in food intake rate [34] leading to fat accumulation and increased body weight.

Tissue	Count	Similar genes (%)	P-Value	Fold Enrichment	Benjamini
Pancreas	20	62.5	1.00E-20	18	3.10E-19
Stomach	7	21.9	5.20E-05	9.9	8.00E-04
Spleen	7	21.9	6.10E-03	4	6.10E-02
Colon	7	21.9	7.30E-03	3.8	5.50E-02
Tongue	4	12.5	9.20E-02	3.6	4.50E-01
* Probe sets showing log fold-changes >1 in the cessation vs. sham comparison were analyzed using DAVID.					

Table 2: DAVID-based* analysis of pancreatic gene signature detected in livers of ApoE$^{-/-}$ mice.

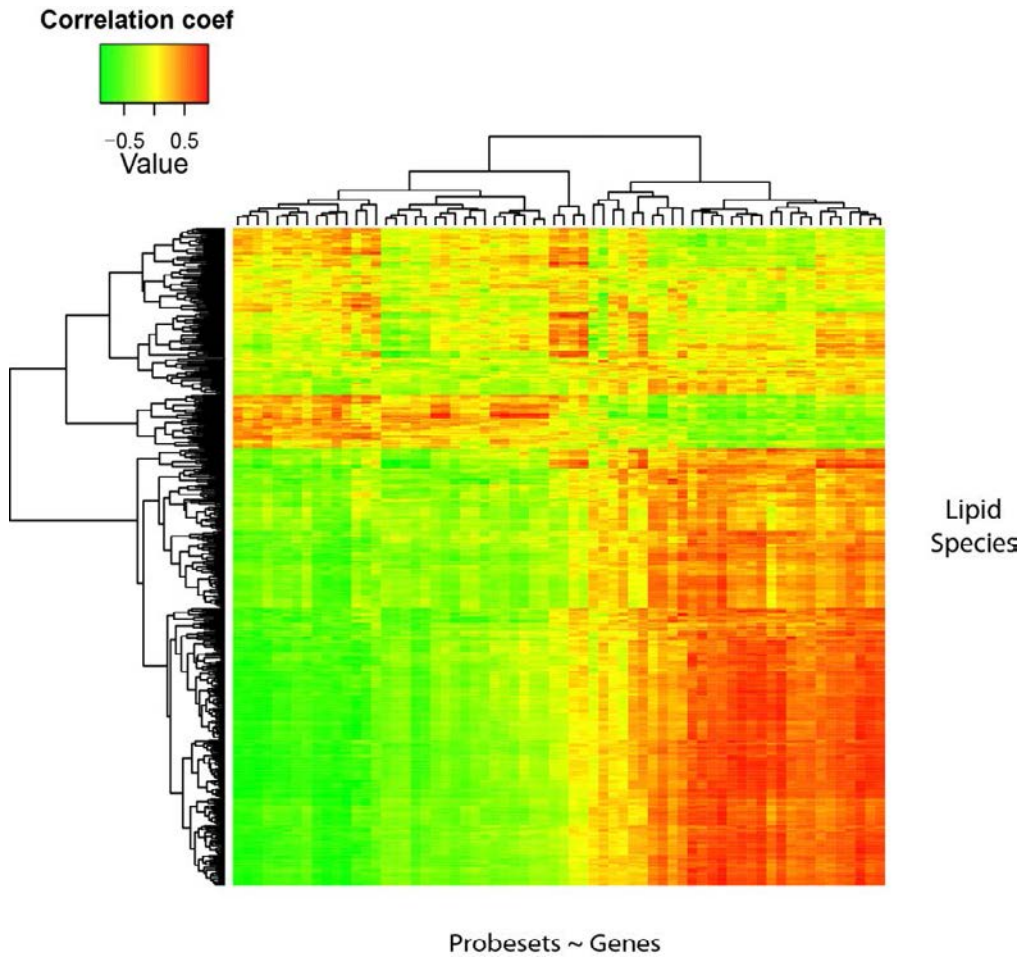

Figure 6: Animal level correlation of hepatic lipidomics and transcriptomics profiles: The heat map represents the correlation coefficients between each probe set on the x-axis and lipid species on the y-axis. Only probe sets showing a correlation coefficient ≥0.8 with a given molecular lipid species were retained in the hierarchical clustering heat map.

Lipidomics analysis of ApoE$^{-/-}$ mice plasma and liver revealed a scenario that is compatible with an increased rate of hepatic lipid accumulation during CS exposure and a reduced retention rate of most lipid classes after smoking cessation

Mass spectrometry-based analysis of livers of CS-exposed ApoE$^{-/-}$ mice resulted in the identification of hundreds of molecular lipid species, most of which are awaiting further mechanistic investigation and biomarker discovery [9].The current report on the effects of smoking cessation on liver's transcriptomics and lipidomics of ApoE$^{-/-}$ mice complements our previous CS exposure findings in liver [9]. Lipid omics analysis in plasma and aorta of ApoE$^{-/-}$ mice suggested a lower lipid accumulation in the smoking cessation group as compared to the continuous smoking group [9,10], whereas results in liver showed a similar decreased pattern for most lipid classes, except TAG. The concentrations of hepatic lipid species including FC and SMs were decreased after smoking cessation, however, a consistently increased concentration of all TAGs was observed in the cessation group compared to sham exposure and continuous CS exposure.

We have previously reported that the plasma levels of TAGs in ApoE$^{-/-}$ mice exposed to CS were lower compared to sham-exposed animals [10],and that plasma levels of VLDL were increased when compared to sham-exposed ApoE$^{-/-}$ mice [9]. No changes were observed in total cholesterol, LDL/IDL or HDL. Despite the increased levels of VLDL, the ApoB 100 lipoprotein carrying the largest levels of TAGs, plasma levels of TAG were decreased in the CS-exposed group. This apparent paradox may be accounted for by differences in lipid composition of other TAG-containing particles (e.g., chylomicron remnants) and their differential contribution to the plasma pool of TAGs.

Transcriptomic analysis of ApoE$^{-/-}$ mice livers suggests that regulation of pathways involved in lipid metabolism account for the hepatic accumulation of TAG

The high concentration of TAGs in the liver after smoking cessation suggests that the removal rate of TAGs is slower compared to other lipid classes. Accumulation of hepatic TAGs is an indicator of fatty liver disease and ApoE$^{-/-}$ mice exhibit nearly twice the levels of TAGs compared to wild type animals [35].Gene expression levels of hepatic enzymes potentially involved in the conversion of monoacylclycerols to TAGs including acyl-CoA synthetases, (Acsl1-5) and TAG synthase (Tgs1) were not up-regulated in the cessation group. Thus, hepatic re-synthesis of TAGs from fatty acids is unlikely. Expression levels of hepatic lipase (Lipg) were not different among the experimental groups either, thus our findings may not be accounted for by a decreased rate of hepatic lipolysis. Finally, the gene expression levels of pancreatic lipase (Pnlip) were highly up-regulated. Thus, putative pancreatic lipase ectopically produced by hepatic cells would have had the opposite effect, namely a reduction in the levels of TAGs. Several molecules involved in fatty acid transport in peroxisomes (e.g. Abcd2 and Abcd4: ATP-binding cassette, sub-family D (ALD), members 2and 4), as well as fatty acid metabolism molecules (e.g., Hsdl2: hydroxysteroid dehydrogenase like 2; Mlycd: malonyl coenzyme A decarboxylase) were clearly correlated with TAGs in our analysis (Figure 6). Taken together, these findings suggest that other mechanisms including increased hepatic transport of TAGs from plasma (e.g., remnants) may account for an increased deposition of TAGs in the liver during smoking cessation.

Eight genes within the lipid metabolism category rendered by the DAVID analysis included Hmgcs2, a mitochondrial HMG-CoA synthase member that is responsible for ketone body synthesis; Abcd2 and Abcd4 (see above), and Elovl3 (elongation of very long chain fatty acids (FEN1/Elo2, SUR4/Elo3)), an enzyme involved in elongation of long fatty acids that provide precursors for synthesis of sphingolipids and ceramides. Elovl3-deficient mice show an impaired ability to accumulate fat [36]. In this context, it is noteworthy that the concentration of TAGs formed by long chain fatty acids (TAG58) were the ones that underwent the largest increases after continuous CS exposure and smoking cessation compared to sham exposure values (Figure 2). It remains to be experimentally tested whether expression of Elovl3 and other fatty acid elongation enzymes have a role in the hepatic accumulation of TAGs containing predominantly long chain fatty acids.

Activation of pathways involved in cell cycle regulation and atherothrombosis were attenuated after smoking cessation in livers of ApoE$^{-/-}$ mice

Gene expression profiling in the liver indicated that a much lower number of genes were differentially regulated in the cessation group compared with the continuous smoking group. When the GSEA for this contrast was conducted with a 10-fold more permissive FDR threshold, the gene sets predicted to increase were linked, with few exceptions, to cholesterol biosynthesis and synthesis of cofactors (CoA, vitamins) involved in lipid metabolism and oxidative phosphorylation, suggesting that hepatic lipid metabolism had reset to control settings. Down-regulation of cell cycle related genes, as well as RNA splicing genes (RC6) was observed after smoking cessation. The significance of these findings is unclear as these sets were not up-regulated after six months of CS exposure. Nicotine, however, has been shown to induce proliferation of hepatic stellate cells leading to liver fibrosis [1]. The down-regulated expression of cell cycle-linked genes might be related to a reduced need to engage cell repair mechanisms after the noxious CS stimulus has been discontinued. Another key finding was the down-regulation of hemostasis-related pathways and genes including those involved in platelet activation. Cigarette smoking is associated with an increased risk of myocardial infarction and known to promote a prothrombotic state in smokers by altering the balance of antithrombotic/prothrombotic factors [37]. Our expression profiling data suggests that smoking cessation may reset that sensitive balance back to physiological levels.

A gene expression signature consistent with exocrine pancreas was activated after CS exposure and smoking cessation in livers of ApoE$^{-/-}$ mice

A sizeable set of pancreatic enzymes including Cbp1, Cela3b and Amy2a and Pnlip were highly up-regulated in livers of ApoE$^{-/-}$ mice exposed to CS. A total of 49 genes within the pancreatic signature exhibiting large changes (log2 folds of 5-13) were detected. Over 60% of all genes are also expressed by pancreas and 22% by other gastrointestinal organs, including stomach and colon. Most of the detected genes are involved in digestive functions. These results suggest that hepatic cells in livers of a fraction of animals differentiated towards a phenotype consistent with pancreatic acinar cells. Sharing of this pancreatic expression profile with other gastrointestinal organs suggest that progenitor cells within the liver parenchyma conserve the capacity to generate cellular phenotypes similar to those of other organs of endodermal origin (e.g., pancreas). Transdifferentiation of hepatocytes into pancreatic acinar cells has been detected in human liver explants [38]. Cellular transdifferentiation may occur in either direction as reprogramming of pancreatic acinar or progenitor cells

to hepatocytes [38-40] or conversion of hepatic cells into pancreatic endocrine cells [41,42]. Evidence for the conversion of hepatocytes to pancreatic acinar cells has been documented in HepG2 and Hepa 1-6 cells [43,44].

Hepatic expression of genes encoding lysosomal enzymes traditionally restricted to pancreas (e.g., chymotrypsin B) suggests that these proteases are involved in hepatic apoptotic pathways [45]. The experimental evidence of exocrine to endocrine transition has provided a theoretical basis to study the plasticity of pancreatic and hepatic cells and their potential therapeutic use in diabetes [46,47]. The pancreatic gene expression signature we observed in livers of ApoE$^{-/-}$ mice appears to be the result of a phenotypic conversion of hepatic cells to a phenotype consistent with exocrine pancreas. Along these lines, livers from rats treated with polychlorinated biphenyls have been shown to develop tissue that was functionally and morphologically identical to pancreatic acinar tissue [48]. Since one animal in the sham group of our study exhibited the pancreatic expression signature, it is conceivable that a small fraction of ApoE$^{-/-}$ mice naturally exhibits this capability while CS exposure increases the rate of this transformation. The detection of the same gene expression pattern in mice from the cessation group indicates that a 3-month cessation period was not sufficient to revert the pancreatic expression pattern induced by three months of CS exposure. Notwithstanding, the current experimental design prevents us from concluding that the observed changes in mice from the cessation group were due solely to CS exposure. Further experiments are required to address this question and the effects of individual smoke constituents, as well as determining whether these phenotypic variants are also present in other mice strains.

In summary, livers of ApoE$^{-/-}$ mice exposed to CS for three months and followed by a three month period of smoking cessation exhibited unique features including accumulation of TAGs and reduction of proatherogenic SMs, as well as a less prothrombotic and atherogenic gene expression profile. Approximately 50% of animals exposed to continuous CS exposure and a smoking cessation protocol displayed a gene expression signature consistent with exocrine pancreas. Additional research should be aimed at understanding the molecular mechanisms involved in the accumulation of TAGs in livers of ApoE$^{-/-}$ mice exposed to CS and smoking cessation.

Acknowledgement

The authors wish to thank Zora Biosciences for the performance of the lipidomics analysis. We would like to acknowledge Marja Talikka and Ignacio Gonzalez Suarez for reviewing the manuscript. We would also like to thank An Berges, Kris Meurrens and Patrick Vanscheeuwijck for the design and realization of the inhalation study, Nadine Schracke for the transcriptomics data generation, and Sam Ansari for the preparation and submission of the transcriptomics data to Array Express.

Funding

The research described in this article was supported by Philip Morris International.

References

1. Kwan HY, Hu YM, Chan CL, Cao HH, Cheng CY, et al. (2013) Lipidomics identification of metabolic biomarkers in chemically induced hypertriglyceridemic mice. J Proteome Res 12: 1387-1398.
2. Du ZY, Degrace P, Gresti J, Loreau O, Clouet P (2011) Vaccenic and elaidic acid equally esterify into triacylglycerols, but differently into phospholipids of fed rat liver cells. Lipids 46: 647-657.
3. Ting TC, Miyazaki-Anzai S, Masuda M, Levi M, Demer LL, et al. (2011) Increased lipogenesis and stearate accelerate vascular calcification in calcifying vascular cells. J Biol Chem 286: 23938-23949.
4. Surgeon_General. Cardiovascular diseases (2010) In: Multiple, ed. How tobacco smoke causes disease: The biology and behavioral basis for smoking-attributable disease: A report of the surgeon general. Atlanta (GA): The Surgeon General 351-434.
5. Price JF, Mowbray PI, Lee AJ, Rumley A, Lowe GD, et al. (1999) Relationship between smoking and cardiovascular risk factors in the development of peripheral arterial disease and coronary artery disease: Edinburgh Artery Study. Eur Heart J 20: 344-353.
6. Sampson UK, Fazio S, Linton MF (2012) Residual cardiovascular risk despite optimal LDL cholesterol reduction with statins: the evidence, etiology, and therapeutic challenges. Curr Atheroscler Rep 14: 1-10.
7. Mora S, Wenger NK, Demicco DA, Breazna A, Boekholdt SM, et al. (2012) Determinants of residual risk in secondary prevention patients treated with high- versus low-dose statin therapy: the Treating to New Targets (TNT) study. Circulation 125: 1979-1987.
8. Nakashima Y, Plump AS, Raines EW, Breslow JL, Ross R (1994) ApoE-deficient mice develop lesions of all phases of atherosclerosis throughout the arterial tree. Arterioscler Thromb 14: 133-140.
9. Boué S, Tarasov K, Jänis M, Lebrun S, Hurme R, et al. (2012) Modulation of atherogenic lipidome by cigarette smoke in apolipoprotein E-deficient mice. Atherosclerosis 225: 328-334.
10. Lietz M, Berges A, Lebrun S, Meurrens K, Steffen Y, et al. (2013) Cigarette-smoke-induced atherogenic lipid profiles in plasma and vascular tissue of apolipoprotein E-deficient mice are attenuated by smoking cessation. Atherosclerosis 229: 86-93.
11. Burns DM, Dybing E, Gray N, Hecht S, Anderson C, et al. (2008) Mandated lowering of toxicants in cigarette smoke: a description of the World Health Organization TobReg proposal. Tob Control 17: 132-141.
12. Terpstra PM, Teredesai A, Vanscheeuwijck PM, Verbeeck J, Schepers G, et al. (2003) Toxicological evaluation of an electrically heated cigarette. Part 4: Subchronic inhalation toxicology. J Appl Toxicol 23: 349-362.
13. Rustemeier K, Demetriou D, Schepers G, Voncken P (1993) High-performance liquid chromatographic determination of nicotine and its urinary metabolites via their 1,3-diethyl-2-thiobarbituric acid derivatives. J Chromatogr 613: 95-103.
14. Vihervaara T, Suoniemi M, Laaksonen R (2013) Lipidomics in drug discovery. Drug Discov Today.
15. Fahy E, Subramaniam S, Murphy RC, Nishijima M, Raetz CR, et al. (2009) Update of the LIPID MAPS comprehensive classification system for lipids. J Lipid Res 50 Suppl: S9-14.
16. Gentleman RC, Carey VJ, Bates DM, Bolstad B, Dettling M, et al. (2004) Bioconductor: Open software development for computational biology and bioinformatics. Genome Biol 5: R80.
17. Smyth GK (2004) Linear models and empirical bayes methods for assessing differential expression in microarray experiments. Stat Appl Genet Mol Biol 3: Article3.
18. Dean CB, Nielsen JD (2007) Generalized linear mixed models: a review and some extensions. Lifetime Data Anal 13: 497-512.
19. Irizarry RA, Hobbs B, Collin F, Beazer-Barclay YD, Antonellis KJ, et al. (2003) Exploration, normalization, and summaries of high density oligonucleotide array probe level data. Biostatistics 4: 249-264.
20. Kuhn MW (2008) Building predictive models in r using the caret package. Classification and regression training Journal of Statistical Software 28.
21. Subramanian A, Tamayo P, Mootha VK, Mukherjee S, Ebert BL, et al. (2005) Gene set enrichment analysis: a knowledge-based approach for interpreting genome-wide expression profiles. Proc Natl Acad Sci U S A 102: 15545-15550.
22. Hermida L, Poussin C, Stadler MB, Gubian S, Sewer A, et al. (2013) Confero: an integrated contrast data and gene set platform for computational analysis and biological interpretation of omics data. BMC Genomics 14: 514.
23. Merico D, Isserlin R, Stueker O, Emili A, Bader GD (2010) Enrichment map: a network-based method for gene-set enrichment visualization and interpretation. PLoS One 5: e13984.
24. Frey BJ, Dueck D (2007) Clustering by passing messages between data points. Science 315: 972-976.
25. Huang da W, Sherman BT, Zheng X, Yang J, Imamichi T, et al. (2009)

Extracting biological meaning from large gene lists with DAVID. Curr Protoc Bioinformatics Chapter 13: Unit 13.

26. Shannon P, Markiel A, Ozier O, Baliga NS, Wang JT, et al. (2003) Cytoscape: a software environment for integrated models of biomolecular interaction networks. Genome Res 13: 2498-2504.

27. Kupershmidt I, Su QJ, Grewal A, Sundaresh S, Halperin I, et al. (2010) Ontology-based meta-analysis of global collections of high-throughput public data. PLoS One 5.

28. Schlage WK, Westra JW, Gebel S, Catlett NL, Mathis C, et al. (2011) A computable cellular stress network model for non-diseased pulmonary and cardiovascular tissue. BMC Syst Biol 5: 168.

29. Westra JW, Schlage WK, Frushour BP, Gebel S, Catlett NL, et al. (2011) Construction of a computable cell proliferation network focused on non-diseased lung cells. BMC Syst Biol 5: 105.

30. Schroeter MR, Sawalich M, Humboldt T, Leifheit M, Meurrens K, et al. (2008) Cigarette smoke exposure promotes arterial thrombosis and vessel remodeling after vascular injury in apolipoprotein E-deficient mice. J Vasc Res 45: 480-492.

31. von Holt K, Lebrun S, Stinn W, Conroy L, Wallerath T, et al. (2009) Progression of atherosclerosis in the Apo E-/- model: 12-month exposure to cigarette mainstream smoke combined with high-cholesterol/fat diet. Atherosclerosis 205: 135-143.

32. Boué S, De León H, Schlage WK, Peck MJ, Weiler H, et al. (2013) Cigarette smoke induces molecular responses in respiratory tissues of Apoe-/- mice that are progressively deactivated upon cessation Atherosclerosis 314: 112-124.

33. Plump AS, Breslow JL (1995) Apolipoprotein E and the apolipoprotein E-deficient mouse. Annu Rev Nutr 15: 495-518.

34. Ypsilantis P, Politou M, Anagnostopoulos C, Tsigalou C, Kambouromiti G, et al. (2013) Effects of cigarette smoke exposure and its cessation on body weight, food intake and circulating leptin, and ghrelin levels in the rat. Nicotine Tob Res 15: 206-212.

35. Wang L, Chen L, Tan Y, Wei J, Chang Y, et al. (2013) Betaine supplement alleviates hepatic triglyceride accumulation of apolipoprotein E deficient mice via reducing methylation of peroxisomal proliferator-activated receptor alpha promoter. Lipids Health Dis 12: 34.

36. Westerberg R, Månsson JE, Golozoubova V, Shabalina IG, Backlund EC, et al. (2006) ELOVL3 is an important component for early onset of lipid recruitment in brown adipose tissue. J Biol Chem 281: 4958-4968.

37. Ambrose JA, Barua RS (2004) The pathophysiology of cigarette smoking and cardiovascular disease: an update. J Am Coll Cardiol 43: 1731-1737.

38. Kuo FY, Swanson PE, Yeh MM (2009) Pancreatic acinar tissue in liver explants: a morphologic and immunohistochemical study. Am J Surg Pathol 33: 66-71.

39. Al-Adsani A, Burke ZD, Eberhard D, Lawrence KL, Shen CN, et al. (2010) Dexamethasone treatment induces the reprogramming of pancreatic acinar cells to hepatocytes and ductal cells. PLoS One 5: e13650.

40. Wallace K, Marek CJ, Hoppler S, Wright MC (2010) Glucocorticoid-dependent transdifferentiation of pancreatic progenitor cells into hepatocytes is dependent on transient suppression of WNT signalling. J Cell Sci 123: 2103-2110.

41. Yang L, Li S, Hatch H, Ahrens K, Cornelius JG, et al. (2002) In vitro trans-differentiation of adult hepatic stem cells into pancreatic endocrine hormone-producing cells. Proc Natl Acad Sci U S A 99: 8078-8083.

42. Perán M, Sánchez-Ferrero A, Tosh D, Marchal JA, Lopez E, et al. (2011) Ultrastructural and molecular analyzes of insulin-producing cells induced from human hepatoma cells. Cytotherapy 13: 193-200.

43. Li WC, Horb ME, Tosh D, Slack JM (2005) In vitro transdifferentiation of hepatoma cells into functional pancreatic cells. Mech Dev 122: 835-847.

44. Darlington GJ, Tsai CC, Samuelson LC, Gumucio DL, Meisler MH (1986) Simultaneous expression of salivary and pancreatic amylase genes in cultured mouse hepatoma cells. Mol Cell Biol 6: 969-975.

45. Miao Q, Sun Y, Wei T, Zhao X, Zhao K, et al. (2008) Chymotrypsin B cached in rat liver lysosomes and involved in apoptotic regulation through a mitochondrial pathway. J Biol Chem 283: 8218-8228.

46. Zhou Q, Brown J, Kanarek A, Rajagopal J, Melton DA (2008) In vivo reprogramming of adult pancreatic exocrine cells to beta-cells. Nature 455: 627-632.

47. Thorel F, Népote V, Avril I, Kohno K, Desgraz R, et al. (2010) Conversion of adult pancreatic alpha-cells to beta-cells after extreme beta-cell loss. Nature 464: 1149-1154.

48. Rao MS, Bendayan M, Kimbrough RD, Reddy JK (1986) Characterization of pancreatic-type tissue in the liver of rat induced by polychlorinated biphenyls. J Histochem Cytochem 34: 197-201.